Isotope Exchange of ND_3 on Pt Catalyst-Loaded 13X Molecular Sieve

Daniel M. Clairmonte [a], Paul R. Beaumont [b]*

Savannah River National Laboratory, Aiken, South Carolina, United States of America

[a]ORCiD: 0009-0006-0824-8387

[b]ORCiD: 0000-0002-8523-1240

*E-mail: paul.beaumont@srnl.doe.gov

Isotope Exchange of ND_3 on Pt Catalyst-Loaded 13X Molecular Sieve

During D-T fusion operations the capture, purification, and recycling of unburned tritium will be crucial, as the formation of tritium containing molecules require additional processing. Removing the tritium can require costly processing to be unbound from the tritium-containing molecules and improvements to these processes will be necessary moving forward. Existing techniques using sorbent material beds to remove tritium-containing molecules from process gas streams undergo repeated high-heat cycling which leads to diminished bed lifespans, necessitating replacement and associated downtime. This work demonstrates the capture and isotopic exchange technique of deuterated ammonia (ND_3), used as a surrogate for tritium, at ambient temperature using a Pt catalyst-loaded 13X molecular sieve. Unmodified 13X molecular sieve is capable of adsorbing and retaining the ND_3 however, incorporation of a catalyst facilitates the isotopic exchange of the hydrogen isotopes. The effluent gas streams were analyzed in conjunction with desorbed ammonia isotopologues post-exchange to verify these results. Isotopically exchanging and removing heavier hydrogen isotopes using this technique provides an alternative to traditional removal methods.

Keywords: ammonia, isotope exchange, 13X, molecular sieve, tritium, fusion

I. INTRODUCTION

Tritium is a critical component in the fuel cycle of a D-T fusion reactor. However, as the majority of tritium supplied to the reactors is unburned,[1,2] there is incentive to capture, purify and recycle it. When dealing with exhaust gases, it is safe to assume that impurities and byproducts will also be exiting the reactor with unburned tritium. Tritiated water (Q_2O) and tritiated ammonia (NQ_3), where Q represents any combination of hydrogen isotopes, are two examples of tritium-containing byproducts that can be captured and processed.[3] To maintain throughput in a future fusion plant and avoid reduced efficiency and downtime, developing effective means to deal with such byproducts becomes important. A common method for removal of tritiated water vapor from effluent gas streams has already been established using sorbent materials.[4,5] However, further

processing to remove the tritium has not been well developed. Efficiently regenerating and maintaining tritium capture materials will play a key role in this process.

Regarding adsorption, one of the simplest systems is an adsorption bed filled with a sorbent material like a zeolite (molecular sieve), as noted above. Zeolites have been extensively studied, finding uses across many industries and in a variety of applications.[6] Water vapor is readily adsorbed by zeolites such as the 13X used in these experiments. Chemicals, including water, become bound to sorbent materials by physisorption or chemisorption.[7,8] To regenerate a traditional zeolite bed external stimuli must be applied with sufficient energy to disrupt both types of interactions. One of the most common ways to accomplish this is by adding heat to the system. Physiosorbed molecules will desorb from the zeolite at lower temperatures and chemisorbed molecules will desorb at higher temperatures. If the zeolite bed is not sufficiently heated, tritium present in the sorbed molecules will remain the zeolite, commonly referred to as a "heel". Having a heel present will also reduce the overall sorption capacity of the material, resulting in reduced operational times and the need for more frequent regenerations to be performed. To correct for this, higher temperatures may be applied to remove the heel, but without the proper heating protocol, there exists a risk of damaging the bed material thus rendering it less effective for future cycles. The same is true for the capture of ammonia. Regardless of what is being captured on the zeolite, sorption of the tritiated molecule is only the first step and the bed will require additional processing to remove the tritium from the bound molecules.

Continuing from research previously performed investigating the isotope exchange performance of a Pt catalyst-loaded 5A zeolite,[9] this work aims to further demonstrate that isotope exchange performed at ambient temperature is a viable replacement to traditional heating of non-catalyst-loaded materials for adsorption and desorption/regeneration applications. This technique has been previously demonstrated where the heavier hydrogen isotopes contained in water (Q_2O) can be exchanged with lighter hydrogen isotopes using a Pt catalyst-loaded material, providing a viable technique for removing water bound tritium.[10,11] This technique would allow for an effluent stream of hydrogen isotopologues (Q_2) that becomes much easier to purify by isotope separation methods. The residual protiated ammonia (NH_3) remaining on the zeolite, which is exceedingly more desirable to remove from process gas streams, may be removed via heated regenerations or disposed of with the bed without concern of a loss of tritium inventory in the sorbent material.

II. EXPERIMENTAL

II.A. Sample Preparation

Samples of 13X molecular sieve (Delta Adsorbents, 8x12 mesh size) were prepared by drying under vacuum at approximately 120 °C prior to use. A wetness impregnation technique was used to load the 13X molecular sieve with platinum catalyst using chloroplatinic acid hexahydrate ($H_2PtCl_6 \cdot 6H_2O$, Sigma-Aldrich) as received, targeting a 1.5 wt% Pt loading. Samples were air-dried overnight then transferred to an oven set at 120 °C for 24 hours. Samples were calcined at 550 °C in static air for approximately 2 hours.

II.B. Analytical and Characterization

Approximately 1 g of sample was loaded into a ½"-OD sample tube with a small amount of quartz wool wadding. A Micromeritics AutoChem II 2920 equipped with a thermal conductivity detector (TCD) and a MKS Cirrus 3 mass spectrometer using ionization energies of 40 eV were used to analyze the samples. In-situ bakeouts, ammonia loading, isotope exchange, Temperature-Programmed-Desorption (TPD), and Temperature-Programmed-Reduction (TPR) experiments were all performed using this analytical configuration. Pressure inside the sample tube was measured at 764 Torr. Standard errors were determined by analyzing samples in triplicate. Brunauer, Emmett and Teller (BET) surface area analyses were performed using a Micromeritics TriStar II Analyzer.

Scanning Electron Microscopy-Energy Dispersive X-ray Analysis (SEM-EDAX) imagining was obtained using a TESCAN MIRA-4 LMU High Resolution (SEM) with Variable Pressure FEG Schottky electron emission source. The SEM has three EDAX detectors and a single-crystal YAG Backscatter Secondary Electron detector. Automated particle analysis was performed by the implementation of the NIST RCA (Rotating Chord Algorithm) in TESCAN scan generator and SharkSEM API protocol.

II.C. Method Development

II.C.1. Bakeout

The in-situ bakeout was performed in a stepwise manner. Helium was passed over the sample at 50 standard cubic centimeters per minute (sccm) during the process. The first step heated

the sample to 125 °C at a rate of 10 °C/min and holding for 60 minutes. Steps two, three, and four utilized the same heating ramp rates and hold times, reaching temperatures of 250, 350, and 450 °C, respectively. Gases exiting the AutoChem were analyzed and recorded throughout this process with the mass spectrometer. After the 60-minute hold at maximum temperature, heating was discontinued and the sample was returned to ambient temperature under a constant He purge.

II.C.2. Ammonia Loading

Once the sample reached ambient temperature the flow would automatically switch over to 30 sccm deuterated ammonia (Nexair, 99.98 atom% D) diluted to 5% with He (Nexair, 99.9999% research grade). This gas mixture would continue to flow, at ambient temperature, for four hours to ensure the capacity of the sample had been exceeded. This process was recorded in real-time by the mass spectrometer, allowing for breakthrough and capacity calculations to be made. To rid the system of any free or loosely bound ammonia on the sample it was purged with He for approximately two hours after ND_3 loading. The relative intensities of the constituents observed during ND_3 loading by the mass spectrometer, normalized against mass 20 (ND_3), have been summarized below in Table 1.

Table 1. ND_3 gas cylinder constituents, relative to ND_3, reported in arbitrary units (a.u.).

Mass	Relative Intensity (a.u.)
2	1.28E-03
3	6.45E-06
4	1.45E-04
17	5.50E-03
18	6.73E-01
19	1.97E-02
20	1.00
28	2.02E-04
32	7.82E-05

II.C.3. Isotope Exchange

Once the two hour He purge had been completed, H_2 (Nexair, 99.9999% research grade) was passed through the sample bed at 30 sccm, at ambient temperature, for 180 minutes until equilibrium had been reached. Equilibrium was defined as the point where the effluent gas

constituent concentrations, recorded by the mass spectrometer, stabilized to the levels observed in the H_2 exchange gas when passed through an empty sample bed. The relative intensities of the constituents observed in the H_2 gas stream used to perform isotope exchange, normalized against mass 2 (H_2), are summarized below in Table 2.

Table 2. H_2 gas cylinder constituents, relative to H_2, reported in arbitrary units (a.u.).

Mass	Relative Intensity (a.u.)
2	1.00
3	5.45E-02
4	1.08E-04
17	1.30E-04
18	5.47E-04
19	7.74E-05
20	3.02E-06
28	2.66E-04
32	2.61E-05

II.C.4. TPD Analysis

Temperature-programmed-desorption was performed by heating samples to 700 °C from ambient temperature at a heating ramp rate of 10 °C/min, including a 60-minute hold time once at temperature. Helium was used as carrier gas and gases desorbed from the sample were recorded in real-time using the mass spectrometer.

II.C.5. TPR Analysis

In a separate set of experiments, samples were subjected to reduction during an in-situ bakeout with a final temperature of 550 °C under constant flow of He at 30 sccm. The samples were returned to room temperature under a constant flow of He at 30 sccm and held there for 20 minutes. The next step was to pass 6% H_2 with a balance of He through the sample bed at 30 sccm while heating to 550 °C with a 2.5 °C/min heating rate. Once the sample reached this temperature it was held for an additional 60 minutes before returning to room temperature. The mass spectrometer was used to record data in real-time, supplementing data obtained via the TCD.

III. RESULTS AND DISCUSSION

SEM-EDS characterization was performed on a sample of Pt/13X, demonstrating its presence on the support material. Two samples, catalyst-free 13X and Pt/13X molecular sieve, began testing with the loading of ND_3. Isotopic exchange was performed on samples that were loaded with ND_3 using H_2 gas. Samples were subjected to TPD analysis after ammonia loading or isotopic exchange and the findings are described below. Samples of 13X and Pt/13X also underwent TPR analysis.

III.A. SEM-EDAX Characterization

SEM-EDAX analysis performed on a sample of Pt/13X, presenting a cross-sectional view of a single sphere. Figure 1 illustrates the Pt layer formed around the outside of the 13X sphere, as shown by the EDAX mapping of Pt denoted by the red coloring overlapping the SEM image of the analyzed sample (left). This was an expected outcome as the shell-core effect is commonly observed when applying this technique of wetness incipient impregnation. Sections of the Pt infused layer of the outer 13X surface measured as thin as 50-100 µm in some areas of the analyzed sample. It should be noted that Pt particles observed within the bulk of the 13X sphere and beyond are incidental to the cross-sectional sample preparation.

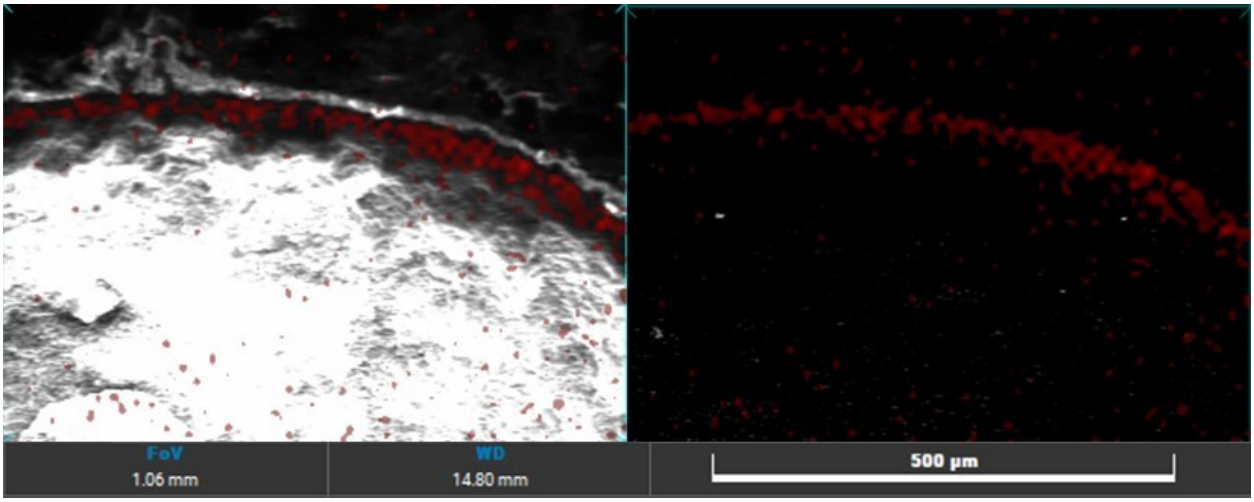

Figure 1. SEM-EDAX spectra of Pt/13X sample.

III.B. Temperature-Programmed-Reduction Analysis

The comparative reduction profiles of the 13X and Pt/13X samples are presented in Figure 2 and Figure 3, respectively. The profile of the 13X sample demonstrated that no reducible species were present on the material. On the other hand, the Pt/13X sample had produced reduction peaks

at approximately 150 minutes (365 °C) and 220 minutes (550 °C). The material was calcined at 550 °C in air as the last step of preparation and was thus assumed to be Pt^0. The first peak, at 150 minutes, indicates formation of water from reduction of PtO_x, indicative of the presence of Pt^{4+} and Pt^{2+}.[12] Though there may be an oxide layer present on the Pt-impregnated support material or indication of deposited Pt interactions with surface or framework oxygens, it does not appear to preclude the aforementioned isotope exchange reaction.

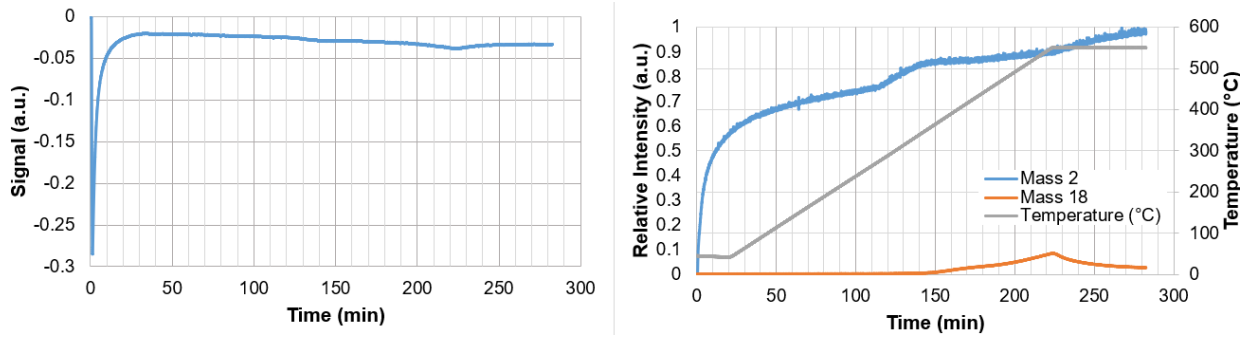

Figure 2. 13X TCD data of reduction profile during TPR analysis (left) and effluent gas stream traces from mass spectrometer (right).

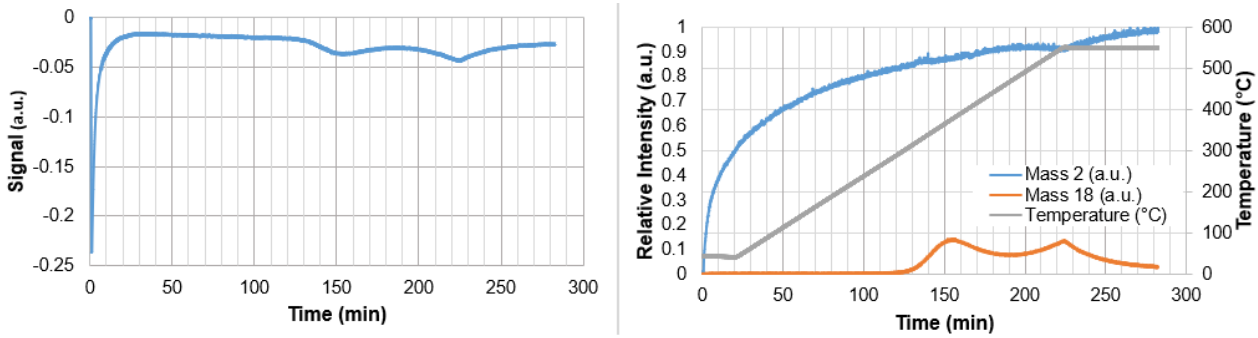

Figure 3. Pt/13X TCD data of reduction profile during TPR analysis (left) and effluent gas stream traces from mass spectrometer (right).

III.C. Bakeout

To ensure the samples were free of water from the atmosphere during handling, an in-situ bakeout was performed before each experiment. Samples were heated to 450 °C in a stepwise manner with constant monitoring of the effluent gas stream by mass spectrometer. The results of the 13X and Pt/13X bakeouts are pictured below in Figure 4. Most of the water on the 13X molecular sieve was desorbed at 250 °C. The Pt/13X trace looks quite different in comparison,

noting a considerable amount of water desorbing at 250 °C along with the bulk of the remaining quantities absorbed to higher energy binding sites desorbing as temperatures reached 350 °C. In either case, both samples appear to have been thoroughly dried up to 450 °C, ensuring that any mass 18 signals present in mass spectrometer data obtained in succeeding experimental steps below 450 °C cannot be ascribed to water.

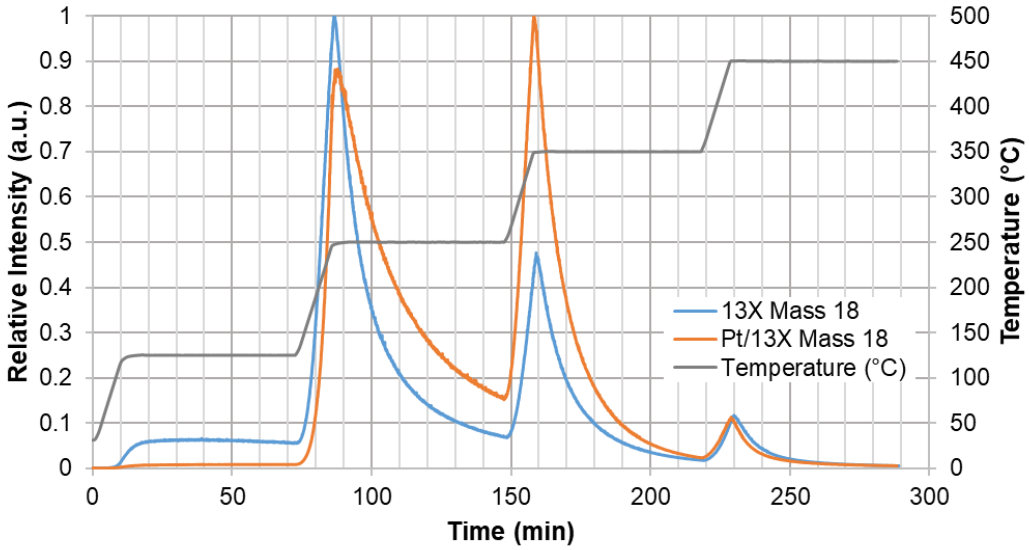

Figure 4. In-situ mass 18 bakeout traces normalized against the highest peak of each trace.

III.D. Ammonia Loading

ND_3 loading began once the bakeout was completed and the sample had cooled to ambient temperature. The time at which full saturation of the sorbent material has occurred is commonly used to calculate loading capacity.[13] However, in some situations it is preferrable to focus on the time at which the sorbate of interest "breaks through", or first registers on the mass spectrometer. The latter approach was implemented here and is shown in Figure 5 and Figure 6. This approach results in more conservative adsorption values and is more accurately referred to as *breakthrough capacity*.[14,15] Results of the loading calculations performed are listed in Table 3, with the Pt/13X sample demonstrating an increase of 0.221 mmol ND_3 per g sample when compared to the 13X sample. This increase was attributed to dative bonding of the ND_3 molecules to vacancies present on Pt atoms. It should also be noted that there was an overall surface area reduction of 63.404 m^2/g for the Pt/13X sample when compared to the 13X sample (Table 3). This reduction was expected as Pt atoms would most likely block pores and channels or otherwise prohibit access to other binding sites within the 13X zeolite.

Table 3. Summary of the calculated ND_3 loading capacities for the 13X and Pt/13X.

Material	Average ND_3 Loading (mmol ND_3/g sample)	Standard Error In 95% CI (±)	Bet Surface Area (m^2/g sample)	Standard Error In 95% CI (±)
13X	5.280	0.129	572.022	7.608
Pt/13X	5.501	0.095	508.618	3.775

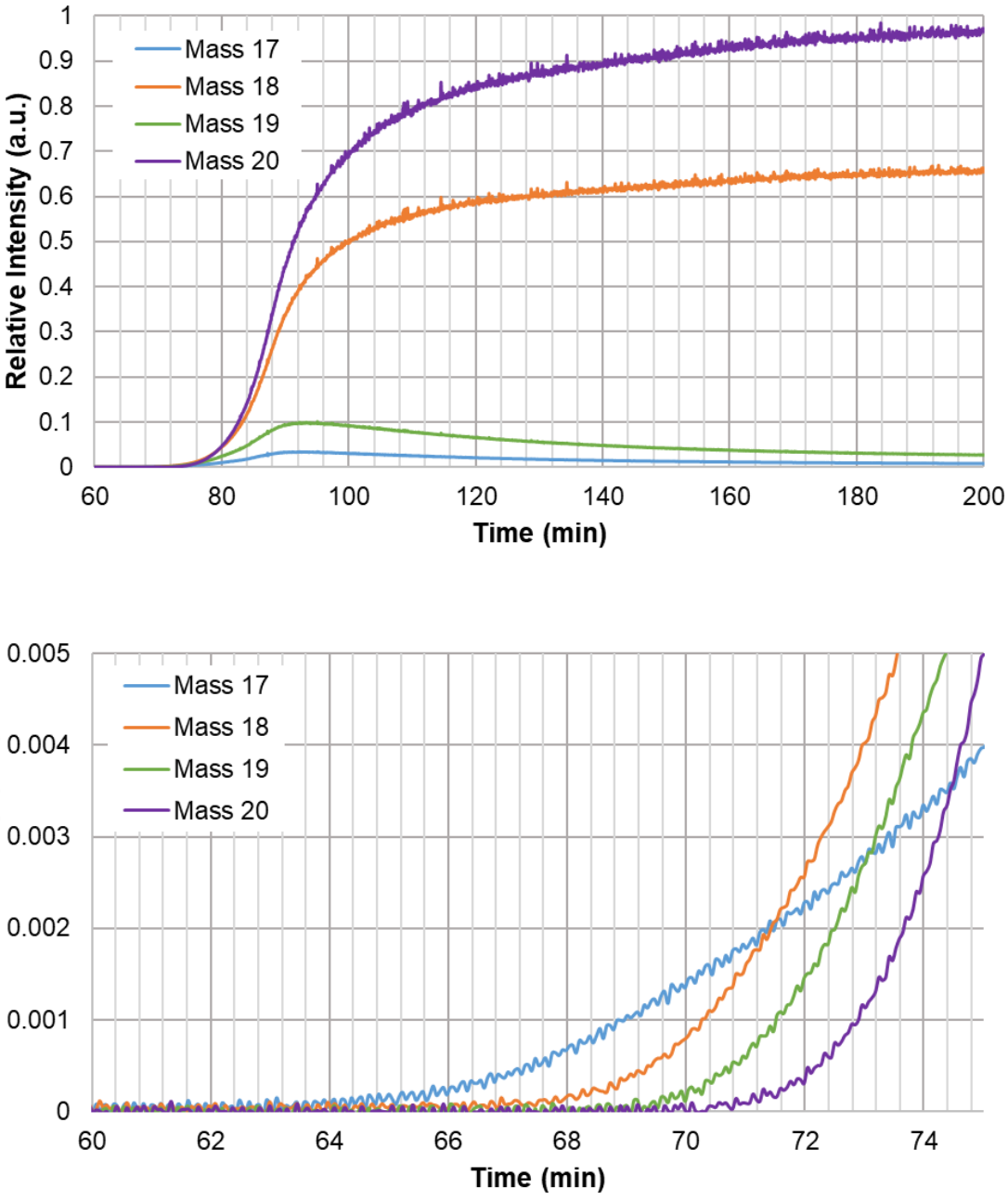

Figure 5. Ammonia loading of the 13X molecular sieve (top) with expanded view of breakthrough (bottom).

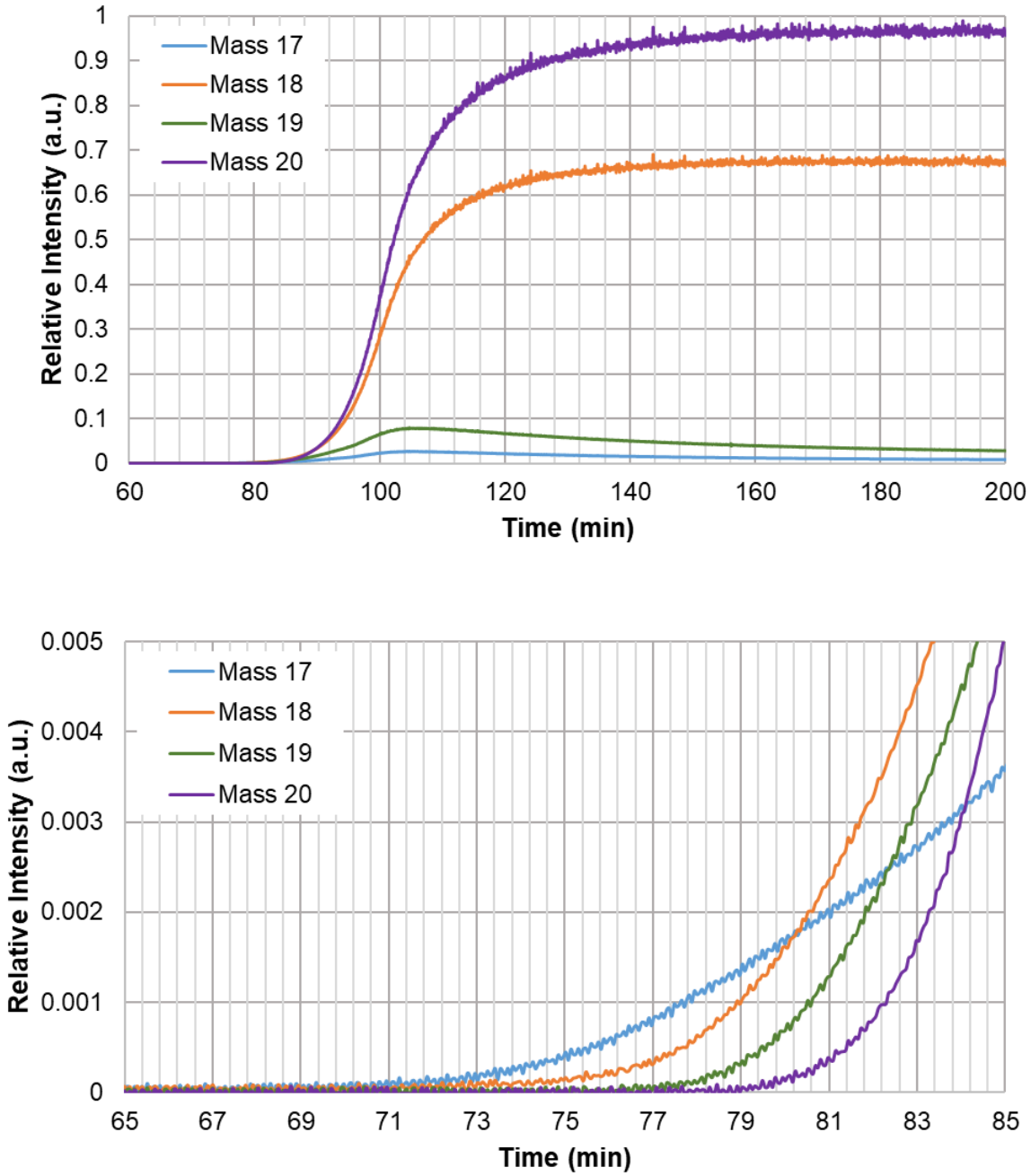

Figure 6. Ammonia loading of the Pt/13X molecular sieve (top) with expanded view of breakthrough (bottom).

During the ND_3 loading process, the four ammonia isotopologues eluted within a few minutes of each other (Figure 5 and Figure 6) in order of mass however, only mass 20 (ND_3) was considered when calculating the ammonia loading capacity. Mass 18 is present in relatively high

concentrations, attributing the majority of its concentration to ND_2^+, a mass fragment of ND_3, also reported in Table 1.[16] As the sample underwent an in-situ bakeout prior to loading, it may be stated with confidence that mass 18 is not water, as mentioned above in the *Bakeout* section.

III.E. Isotope Exchange

Isotope exchange experiments were performed after ammonia loading. Figure 7 and Figure 8 show the effluent streams from the 13X and Pt/13X, respectively, as recorded by MS. Figure 7 shows H_2 and HD (masses 2 and 3) immediately passing through the sample bed and equilibrating. HD (mass 3) presence is expected as deuterium is present in the H_2 cylinder used (Table 2). The presence of ND_3 and ND_2^+ (masses 20 and 18) can most likely be explained as the loosely bound ammonia molecules that were weakly physisorbed to the sample exiting the bed. Of most interest is the static nature of the HD and D_2 traces (masses 3 and 4). H_2 is unable to dissociate and thus exchange with the heavier isotope without the Pt catalyzing the reaction, explaining why an increase in masses 3 and 4 is not observed.[17,18]

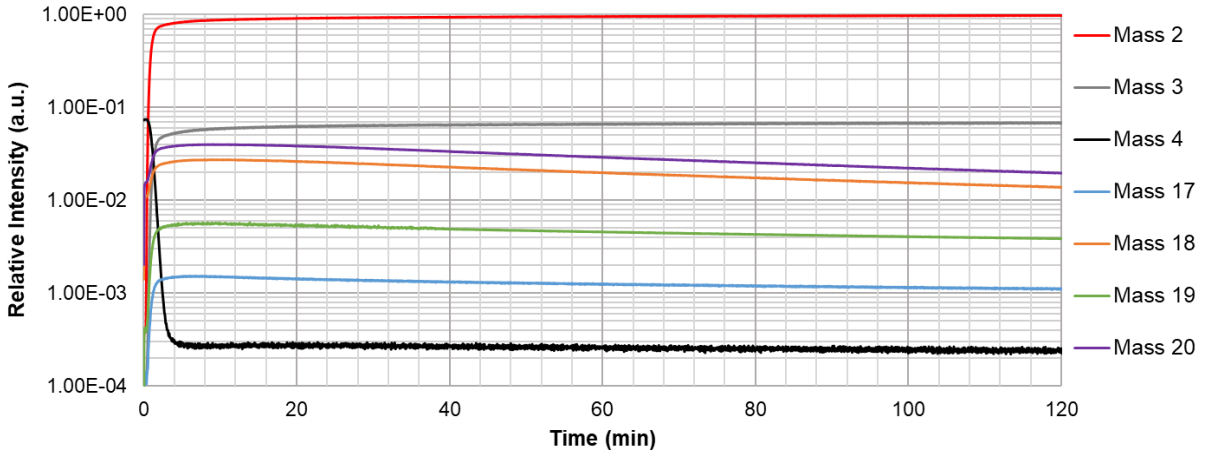

Figure 7. Isotope exchange curve for the 13X sample.

This proposed mechanism for the isotope exchange is based on a "hydrogen spillover" type mechanism.[17-19] By definition, the terminology used to define *spillover* cannot accurately be used to describe this interaction in which H atoms (proton with electron) move from the Pt metal to the support material due to the 13X being a nonreducible surface.[17] The difference being that after dissociative chemisorption of the H_2 occurs on the metal surface, the H atom then migrates to the

surface of a reducible support material. As the 13X is a nonreducible support material, as demonstrated by the comparative TPR spectra (Figure 2), the H migrates from the Pt to the support surface as a proton (H^+) which is then able to isotopically exchange for D of the chemisorbed ND_3.[17] It has also been reported that the transfer of the H^+ occurs at the metal-support interface and the method of migration is facilitated by the H-D exchange of migrating hydrogen isotope cations with hydroxyl groups (O-H and/or O-D) of the support surface.[17,19] The proposed overall mechanism occurs in the following steps, as it applies to this series of experiments. Ammonia is first sorbed onto the support material via physi- and chemisorption interactions.[20,21] Incoming molecular H_2 dissociates on the surface of the Pt and the H^+ begin to diffuse on to the support material surface. Migrating H^+ encounter the sorbed ND_3 molecules where the isotope exchange occurs. The exchanged deuteron (D^+) relocates to the surface of the support material and recombines with other hydrogen isotope cations collected on the surface to be desorbed as HD or D_2. The mechanism for recombination and desorption of the molecular hydrogen isotopologues is suspected to take place on the Pt particles or within the vicinity of the Pt-support material interface. It should be noted that the electrons, once removed from the incoming H_2, can only be retained on the metal, in cases where nonreducible support materials are used.[18]

Supporting the proposed mechanism where incoming H_2 dissociates on the surface of the Pt and ultimately exchanges with the bound ND_3, Figure 8 shows clear isotopic exchange behavior using the Pt/13X sample as evidenced by the mass 3 and 4 traces, noting the importance of incorporating a catalyst to facilitate the process. As H_2 passes through the sample bed it exchanges sample-bound deuterium for hydrogen, forming both HD and D_2 (masses 3 and 4). Each of these traces show an immediate increase which settles closer to equilibrium concentrations of the H_2 exchange gas with time (see Table 2). Masses 18, 19, and 20 are all more dynamic than what is observed in the 13X sample effluent (Figure 7). Weakly bound ND_3 is found leaving the sample bed again however, it is being converted to ND_2H, NDH_2, and NH_3. It is suspected that these isotopologues were formed as the loosely bound ND_3 moved over the Pt and interacted with the abundance of H_2 molecules nearby, or displaced partially exchanged ammonia molecules from the support material surface.[3] Masses 19, 18, and 17 sequentially decrease in concentration, further indicating the hydrogen isotope exchange.

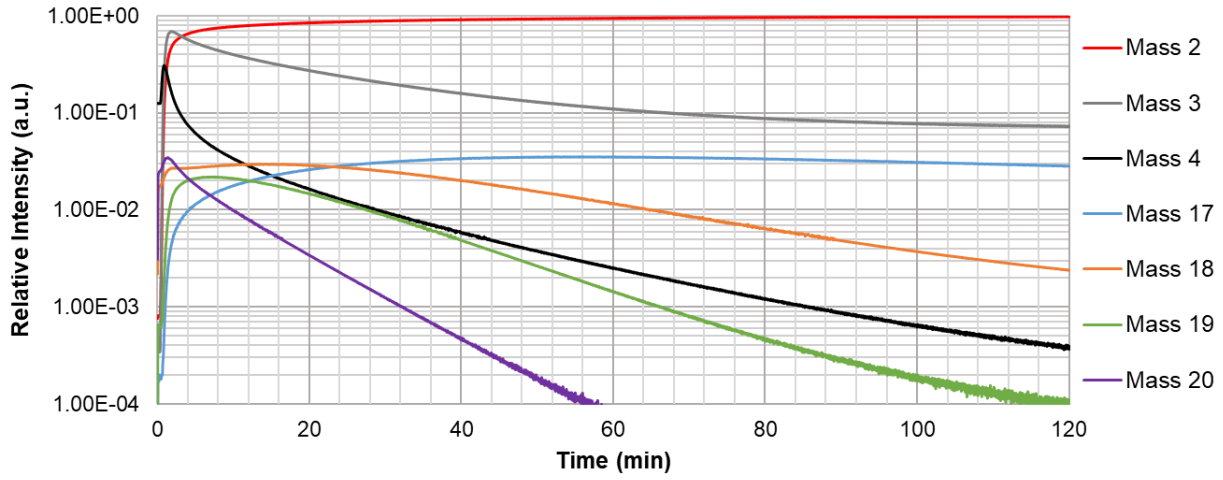

Figure 8. Isotope exchange curve for the Pt/13X sample.

III.F. Temperature-Programmed-Desorption Analysis

The 13X and Pt/13X samples were subjected to temperature-programmed desorption analysis to verify that isotope exchange occurred. The TPD spectra of both samples verify that ammonia was adsorbed and retained by the zeolites. The 13X sample trace (Figure 9) shows that mass 20 is the primary desorbing species, followed by mass 18. Had isotope exchange occurred using the 13X sample, mass 17 would be present in much higher concentrations.

Regardless of the isotopologue, the bulk of the ammonia desorption occurred at approximately 200 °C. A small amount of ammonia remained on the sample up to 500 °C, as seen in Figure 9. These remnants of ammonia are bound to higher energy binding sites and require more thermal energy to desorb from the material. Without the proper heating regimen these heels of ammonia will reduce adsorption capacity for subsequent cycles and pose a challenge to inventory allowances (when tritiated). This poses an additional consideration in that as zeolite is subjected to higher temperatures, the closer to “end-of-life” conditions the zeolite becomes.

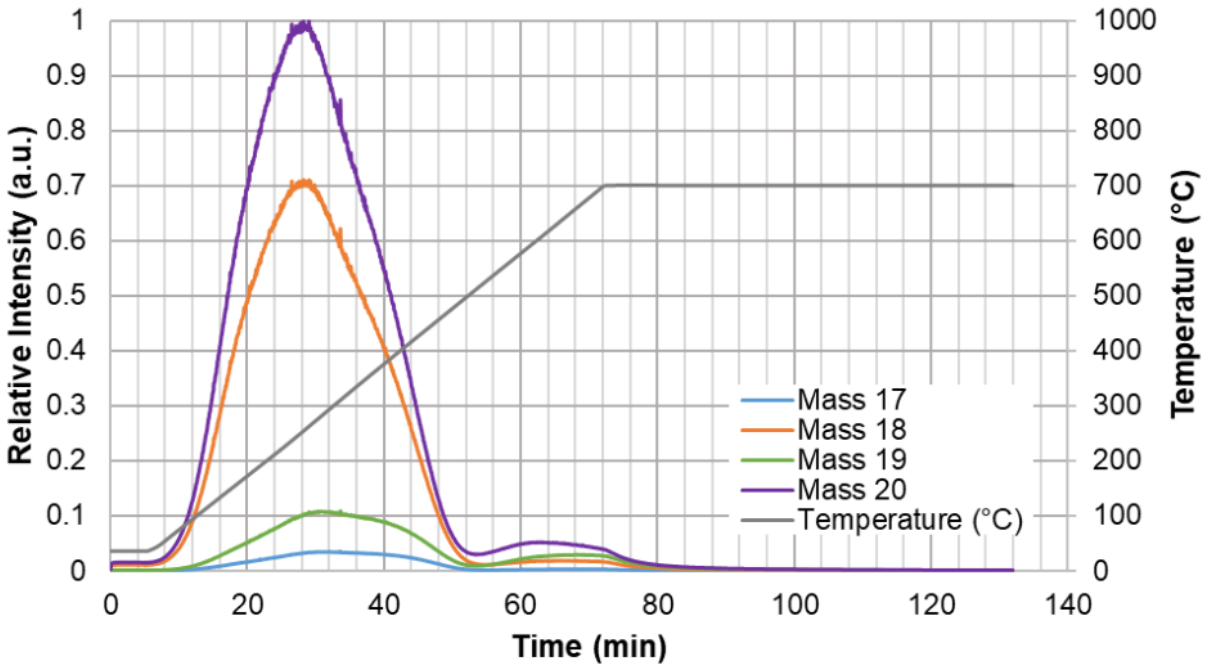

Figure 9. TPD spectra of the 13X sample.

On the other hand, the Pt/13X sample (Figure 10) was able to isotopically exchange almost all of the ND_3 for NH_3. Except for mass 17, the only other isotopologue desorbed was mass 18, presumed to be NH_2D due to the lack of available ND_3 for fragmentation. Additionally, in contrast to the 13X sample, NH_3 had nearly completely desorbed before reaching 550 °C. This would suggest that having Pt catalyst aids in the complete removal of NH_3 at lower temperatures, providing added protection in avoiding the expedited degradation of the support material resulting from heating to "end-of-life" conditions to remove any residual heels.

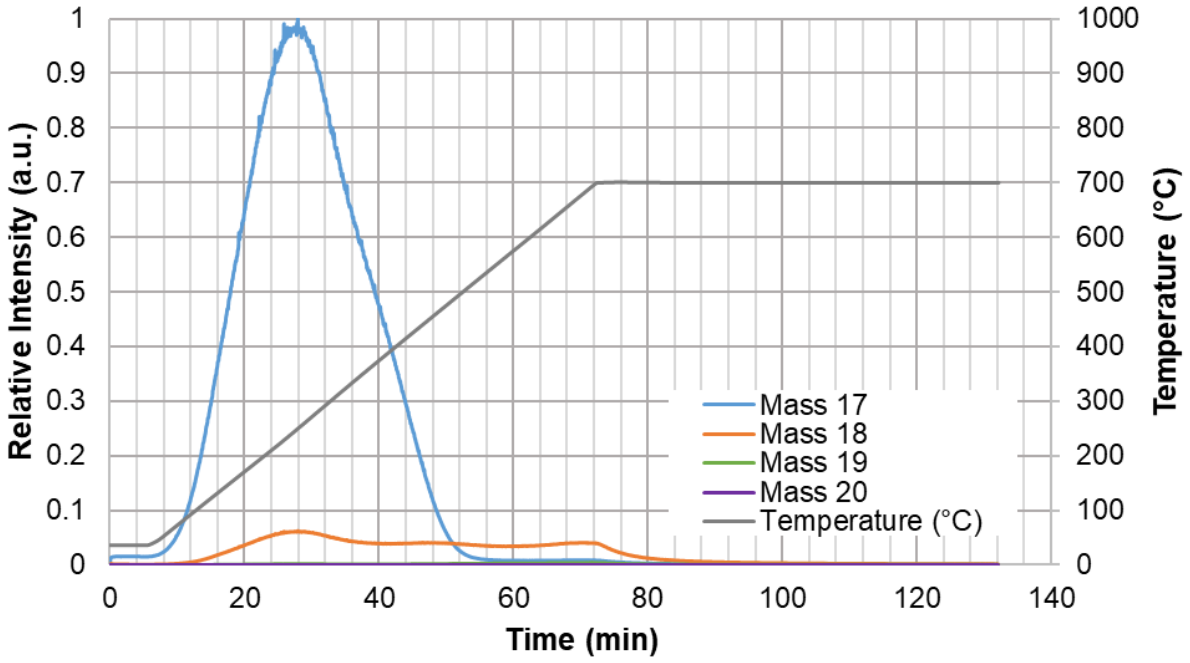

Figure 10. TPD spectra of the Pt/13X sample.

IV. CONCLUSION

This work demonstrates the benefits of incorporating a Pt catalyst for the successful isotopic exchange of ammonia isotopologues at ambient temperature using hydrogen gas. While both 13X and Pt/13X are capable of adsorption and retention of ND_3, the Pt/13X sample demonstrates higher capacity and the ability to isotopically exchange due to its preference for the lighter hydrogen isotope.

Acknowledgements

The author would like to acknowledge Donna W. Allison for her assistance in material preparation and experimentation, and Daniel Morrall for SEM-EDAX analysis. This work was produced by Battelle Savannah River Alliance, LLC under contract 89303321CEM000080 with the U.S. Department of Energy (DOE).

Declaration of competing interest

The authors declare that they have no known competing financial interests or personal relationships that could have appeared to influence the work reported in this paper.

References

(1) Hirooka, Y., *Fusion Science and Technology*, **2007**, *52*, 1040-1044.
(2) Nishikawa, M., *Fusion Science and Technology*, **2010**, *57*, 120-128.
(3) Antunes, R.; Steiner, R.; Marot, L.; Meyer, E., *International Journal of Hydrogen Energy*, **2022**, *47*, 14130-14140.
(4) Nakashima, M.; Tachikawa, E., *Journal of Nuclear Science and Technology*, **1982**, *19*, 571-577.
(5) Kim, K.R.; Lee, M.S.; Paek, S.; Yim, S.P.; Ahn, D.H.; Chung, H., *Radiation Physics and Chemistry*, **2007**, *76*, 1493-1496.
(6) Bingre, R.; Louis, B.; Nguyen, P., *Catalysts*, **2018**, *8*, 163.
(7) Sayılgan, Ş.Ç.; Mobedi, M.; Ülkü, S., *Microporous and Mesoporous Materials*, **2016**, *224*, 9-16.
(8) Thommes, M.; Kaneko, K.; Neimark, A.V.; Olivier, J.P.; Rodriguez-Reinoso, F.; Rouquerol, J.; Sing, K.S.W., *Pure and Applied Chemistry*, **2015**, *87*, 1051-1069.
(9) Beaumont, P.R.; Clairmonte, D.M., *Fusion Science and Technology*, **2024**, 1-7.
(10) Ruiz-Yi, B.; Angelette, L.M.; Beaumont, P.R., *Fusion Science and Technology*, **2024**, *80*, 48-54.
(11) Enoeda, M.; Higashijima, T.; Nishikawa, M.; Mitsuishi, N., *Journal of Nuclear Science and Technology*, **1986**, *23*, 1083-1093.
(12) Huizinga, T.; Van Grondelle, J.; Prins, R., *Applied Catalysis*, **1984**, *10*, 199-213.
(13) Topsøe, N.-Y.; Pedersen, K.; Derouane, E.G., *Journal of Catalysis*, **1981**, *70*, 41-52.
(14) Helminen, J.; Helenius, J.; Paatero, E.; Turunen, I., *Journal of Chemical & Engineering Data*, **2001**, *46*, 391-399.
(15) Inglezakis, V.J., *Journal of Colloid and Interface Science*, **2005**, *281*, 68-79.
(16) Mann, M.M.; Hustrulid, A.; Tate, J.T., *Physical Review*, **1940**, *58*, 340-347.
(17) Prins, R., *Chemical Reviews*, **2012**, *112*, 2714-2738.
(18) Wu, S.; Tseng, K.-Y.; Kato, R.; Wu, T.-S.; Large, A.; Peng, Y.-K.; Xiang, W.; Fang, H.; Mo, J.; Wilkinson, I.; Soo, Y.-L.; Held, G.; Suenaga, K.; Li, T.; Chen, H.-Y.T.; Tsang, S.C.E., *Journal of the American Chemical Society*, **2021**, *143*, 9105-9112.
(19) Miller, J.T.; Meyers, B.L.; Barr, M.K.; Modica, F.S.; Koningsberger, D.C., *Journal of Catalysis*, **1996**, *159*, 41-49.
(20) Farneth, W.E.; Gorte, R.J., *Chemical Reviews*, **1995**, *95*, 615-635.
(21) Niwa, M.; Katada, N., *The Chemical Record*, **2013**, *13*, 432-455.